



# From Biomass Waste to Functional Iron Oxides: Mechanistic Understanding, Structure Engineering, and Environmental Applications

Dewi Kurnianingsih Arum Kusumahastuti<sup>1\*</sup>, November R. Aminu<sup>1</sup>, Agung R. Gintu<sup>2</sup>, Emmanuel Hernanda Yustisia Susanto<sup>1</sup>, Gecia Ovi Wulandari<sup>1</sup>

<sup>1</sup>Department Chemistry, Faculty of Science and Mathematics, Satya Wacana Christian University, Salatiga, Indonesia.

<sup>2</sup>Master of Agricultural Sciences, Faculty of Agriculture and Business, Satya Wacana Christian University, Salatiga, Indonesia.

Received: March 09, 2026

Revised: May 09, 2026

Accepted: June 25, 2026

Published: June 30, 2026

Corresponding Author:

Dewi Kurnianingsih Arum Kusumahastuti

[dewi.hastuti@uksw.edu](mailto:dewi.hastuti@uksw.edu)

DOI: [10.29303/jppipa.v12i6.14780](https://doi.org/10.29303/jppipa.v12i6.14780)

 Open Access

© 2026 The Authors. This article is distributed under a (CC-BY License)



**Abstract:** Biomass-mediated green synthesis of iron oxide nanomaterials has gained increasing attention as a sustainable alternative to conventional chemical methods, offering lower energy requirements, reduced chemical toxicity, and intrinsic surface functionalization. Unlike previous reviews that mainly summarize synthesis routes or environmental applications separately, this review establishes an integrated structure-property-performance framework to systematically correlate biomass chemistry, phase evolution, and functional remediation behavior of iron oxide nanomaterials. A structured scoping review was conducted by analyzing 42 peer-reviewed articles published between 2010 and 2024, selected from major scientific databases using predefined inclusion criteria emphasizing crystalline phase identification, quantitative structural characterization, and measurable environmental performance. Comparative synthesis of the collected data reveals that phytochemical constituents, particularly polyphenols and organic acids, regulate Fe<sup>3+</sup> reduction, chelation equilibria, nucleation kinetics, and phase selectivity among Fe<sub>3</sub>O<sub>4</sub>, γ-Fe<sub>2</sub>O<sub>3</sub>, and α-Fe<sub>2</sub>O<sub>3</sub>. Fe<sub>3</sub>O<sub>4</sub>-rich systems exhibited smaller particle sizes (10–30 nm), higher saturation magnetization (30–70 emu g<sup>-1</sup>), and superior pollutant removal efficiencies (90–99%), while γ-Fe<sub>2</sub>O<sub>3</sub> showed moderate magnetic properties (20–50 emu g<sup>-1</sup>) and α-Fe<sub>2</sub>O<sub>3</sub> displayed larger particle sizes (30–60 nm), lower magnetization (<2 emu g<sup>-1</sup>), but greater thermodynamic stability. Adsorption capacities ranged from 30–250 mg g<sup>-1</sup> depending on pollutant type and phase composition. Despite these promising performances, variability in biomass composition, phase instability, and inconsistent testing protocols remain major barriers to reproducibility and scalability. This review provides a quantitative and mechanistic framework to guide rational synthesis design, improve reproducibility, and accelerate scalable deployment of biomass-derived iron oxide nanomaterials for environmental remediation.

**Keywords:** Biomass-mediated synthesis; Fenton catalysis; Heavy metal removal; Iron oxide nanoparticles; Phytochemical reduction

## Introduction

The remarkable physicochemical properties, cost-effectiveness, and versatile applicability of iron oxide

nanomaterials across environmental, biomedical, and energy-related disciplines have garnered sustained scientific attention over the past two decades (Alex Mbachu et al., 2023). Due to their distinctive magnetic behavior, chemical stability, and surface reactivity,

### How to Cite:

Kusumahastuti, D. K. A., Aminu, N. R., Gintu, A. R., Susanto, E. H. Y., & Wulandari, G. O. (2026). From Biomass Waste to Functional Iron Oxides: Mechanistic Understanding, Structure Engineering, and Environmental Applications. *Jurnal Penelitian Pendidikan IPA*, 12(6), 146–155. <https://doi.org/10.29303/jppipa.v12i6.14780>

Magnetite ( $\text{Fe}_3\text{O}_4$ ), Hematite ( $\alpha\text{-Fe}_2\text{O}_3$ ), and Maghemite ( $\gamma\text{-Fe}_2\text{O}_3$ ) are the most extensively studied of the numerous iron oxide phases (Shabatina et al., 2020; Yousif et al., 2023). Superparamagnetic nanoscale magnetite makes magnetic separation and recovery easy, which is ideal for environmental remediation (Devi et al., 2019).

The size and crystalline phase of iron oxide nanoparticles can be controlled to a relatively small degree using conventional synthesis methods such as microemulsion, thermal decomposition, sol-gel, co-precipitation, and hydrothermal treatment (Nehe & Kulkarni, 2025). Nevertheless, these techniques frequently necessitate hazardous reducing and stabilizing agents, toxic organic solvents, elevated reaction temperatures, and high energy consumption. These deficiencies are in direct opposition to the increasing global emphasis on environmentally responsible material production and sustainable chemistry (Xu et al., 2022).

A paradigm transition in nanomaterial fabrication is represented by the emergence of green synthesis approaches. Green synthesis, on the other hand, uses biological systems or substances that come from nature as reducing, chelating, and stabilizing agents instead of chemicals. Most of the time, early studies used fresh plant extracts. But more recent studies have concentrated on biomass waste materials, such as agricultural leftovers, food processing by-products, fruit peels, spent coffee grounds, lignocellulosic waste, and other agro-industrial discards. This change is in line with the ideas of a circular economy, which turns low-value waste streams into useful nanomaterials that are good for the environment and the economy (Kumar et al., 2023).

A complex matrix of phytochemicals, such as polyphenols, flavonoids, tannins, lignin derivatives, carbohydrates, proteins, and organic acids, is present in biomass waste. Functional groups such as hydroxyl, carbonyl, and carboxyl moieties in these chemicals can contribute electrons, chelate iron ions, and stabilize the surfaces of nanoparticles. Biomass waste serves as both a reducing and capping agent, optimizing synthesis reactions and minimizing the necessity for additional stabilizers (Demirezen et al., 2022). However, the molecular processes that control the reduction of iron ions, nucleation, and phase evolution are still not well understood. Variability in biomass content, extraction conditions, and reaction parameters exacerbates the challenges of repeatability and scalability (Parveen et al., 2025).

Biomass-mediated iron oxide nanomaterials have exhibited promising performance in environmental remediation, particularly in the areas of heavy metal adsorption, pigment degradation, Fenton-like catalysis,

and photocatalysis. This is from an application perspective. The magnetic separability of  $\text{Fe}_3\text{O}_4$ -based systems improves operational efficiency and recyclability, but surface functionalization by residual biomolecules may affect adsorption capacity and catalytic activity. Even with these improvements, the literature still doesn't provide a complete synthesis of mechanistic understanding, structure-property correlations, and sustainability considerations.

Despite the increasing number of studies on biomass-mediated synthesis of iron oxide nanomaterials, the current body of knowledge remains highly fragmented, with most reports focusing independently on synthesis procedures, material characterization, or application performance. This fragmented understanding limits the ability to establish predictive relationships between biomass chemistry, nanoparticle structure, and environmental functionality. Such a gap is scientifically important because iron oxide phase composition ( $\text{Fe}_3\text{O}_4$ ,  $\gamma\text{-Fe}_2\text{O}_3$ , and  $\alpha\text{-Fe}_2\text{O}_3$ ) directly governs key functional properties including redox activity, magnetic recoverability, adsorption affinity, and catalytic efficiency. Without a mechanistic understanding of these interdependencies, reproducibility remains low and rational scale-up for practical environmental deployment remains difficult.

The novelty of this review lies in constructing an integrated structure-property-performance framework specifically for biomass-derived iron oxide nanomaterials, an aspect that has not been systematically addressed in previous reviews. Unlike earlier studies that mainly summarize synthesis methods or environmental applications separately, this review critically correlates phytochemical-mediated reduction mechanisms, phase-selective crystal formation, and quantitative remediation performance across different iron oxide systems. This integrated perspective is particularly important in the context of sustainable nanotechnology, where biomass variability significantly affects material consistency and functional reliability.

Therefore, this review provides a critical and comprehensive analysis of biomass waste-assisted green synthesis of iron oxide nanomaterials, focusing on (i) the molecular mechanisms of biomass-mediated reduction and stabilization, (ii) the influence of synthesis parameters on phase evolution, particle size, and magnetic behavior, (iii) comparative environmental performance in adsorption and Fenton-like catalysis, and (iv) the major reproducibility challenges and standardization gaps that must be addressed for scalable and environmentally responsible applications. By consolidating these aspects, this review aims to provide a predictive foundation for rational material design and accelerate the development of biomass-based iron oxide

nanotechnology within green chemistry and circular material systems.



**Figure 1.** Conceptual overview of biomass-mediated synthesis of iron oxide nanomaterials, highlighting the role of phytochemical compounds in controlling  $Fe^{3+}/Fe^{2+}$  redox reactions, phase formation, and magnetic properties, as well as their environmental applications in heavy metal adsorption and Fenton-like catalytic degradation

## Method

This review was conducted following a structured scoping review approach adapted from the PRISMA-ScR (Preferred Reporting Items for Systematic Reviews and Meta-Analyses extension for Scoping Reviews) guidelines to ensure transparency, reproducibility, and systematic data synthesis (Tricco et al., 2018). Literature retrieval was performed using three major scientific databases: Scopus, Web of Science, and Google Scholar, covering publications from 2010 to 2024. The search strategy employed combinations of keywords including “biomass-mediated iron oxide nanoparticles,” “green synthesis” AND “ $Fe_3O_4/Fe_2O_3$ ,” “plant extract” AND “iron oxide nanomaterials,” and “Fenton-like reaction” AND “biogenic iron oxide.”

The initial search yielded 214 articles. After removal of duplicates ( $n = 46$ ), 168 records were screened based on title and abstract relevance. Of these, 103 articles were excluded due to insufficient relevance, leaving 65 full-text articles for eligibility assessment. Finally, 42 peer-reviewed studies were included for qualitative and comparative analysis based on predefined inclusion criteria. Eligible studies were required to: (i) report biomass-assisted synthesis of iron oxide nanomaterials, (ii) clearly identify crystalline phases ( $Fe_3O_4$ ,  $\gamma-Fe_2O_3$ , or  $\alpha-Fe_2O_3$ ), (iii) provide quantitative structural

characterization such as particle size or magnetization, and (iv) evaluate environmental applications including adsorption or catalytic degradation. Studies involving purely chemical synthesis without biomass participation or lacking quantitative characterization were excluded.

Extracted data included biomass source, synthesis parameters (pH, temperature, reaction time), crystalline phase, particle size distribution, saturation magnetization, adsorption capacity, and catalytic degradation efficiency. Data were synthesized using comparative thematic analysis to identify mechanistic trends and establish structure–property–performance relationships among different biomass-derived iron oxide systems.

## Result and Discussion

### *Mechanistic Formation Pathways and Phase Control*

Biomass-mediated synthesis of iron oxide nanomaterials is governed by coupled redox, coordination, and hydrolysis equilibria (Tiwari et al., 2026). Polyphenolic compounds and lignin-derived aromatics donate electrons to  $Fe^{3+}$ , partially reducing it to  $Fe^{2+}$  via proton-coupled electron transfer mechanisms (Hu et al., 2025). This gradual reduction distinguishes green synthesis from classical alkaline co-precipitation, where instantaneous supersaturation induces burst nucleation. Controlled  $Fe^{2+}$  generation regulates mixed-valence magnetite ( $Fe_3O_4$ ) formation, while insufficient reduction or prolonged oxidation favors  $\gamma-Fe_2O_3$  and ultimately  $\alpha-Fe_2O_3$ .

Chelation by carboxylate and phenolate groups forms Fe–organic complexes that modulate free ion activity and nucleation kinetics (Malacaria et al., 2021). Strong coordination may suppress  $Fe^{2+}$  formation and shift thermodynamic preference toward  $\alpha-Fe_2O_3$ . In contrast, moderate complexation supports  $Fe^{2+}/Fe^{3+}$  coexistence and stabilizes  $Fe_3O_4$  during early growth stages.

Typical synthesis conditions reported across studies include pH 7–11 and temperatures between 25–90°C. Particle sizes generally range from 10–60 nm, reflecting moderated supersaturation and surface passivation effects. Post-synthesis oxidation remains a critical determinant of final phase identity, particularly under aerobic drying or calcination.

**Table 1.** Synthesis Conditions and Structural Characteristics

Biomass Source	Temp (°C)	pH	Phase	Size (nm)	Ms ( $emu\ g^{-1}$ )
Tea waste (Periakaruppan et al., 2021)	60–80	8–10	$Fe_3O_4$	12–25	52–68
Fruit peel (Abdullah et al., 2024; Khan et al., 2025)	70–90	9–11	$\gamma-Fe_2O_3$	15–35	30–45
Rice husk (Castillo et al., 2021)	400 (calcined)	–	$\alpha-Fe_2O_3$	30–80	<2

Magnetite-dominant systems exhibit significantly higher saturation magnetization (30–70  $emu\ g^{-1}$ )

compared to hematite (<2  $emu\ g^{-1}$ ), confirming the strong phase–magnetic property correlation.

### Structure–Property Relationships

Crystalline phase, particle size, defect density, and surface functionalization collectively determine environmental functionality.

Fe<sub>3</sub>O<sub>4</sub> possesses an inverse spinel structure enabling Fe<sup>2+</sup>/Fe<sup>3+</sup> electron hopping, which enhances redox-driven catalytic reactions (Dong et al., 2022; P. Wang et al., 2017). γ-Fe<sub>2</sub>O<sub>3</sub>, lacking structural Fe<sup>2+</sup>, shows lower intrinsic redox flexibility but retains magnetic separability (Ramos-Guivar et al., 2021). α-Fe<sub>2</sub>O<sub>3</sub> provides superior oxidative stability but limited Fenton-like activity (Magomedova et al., 2023).

Superparamagnetism is typically observed below ~20–25 nm, allowing rapid magnetic recovery without remanence. However, surface organic coatings reduce magnetization due to non-magnetic mass contribution and surface spin canting (Tyagi et al., 2023). Oxygen vacancies and Fe<sup>2+</sup>-rich domains enhance catalytic turnover by facilitating electron transfer (W. Wang et al., 2021). Conversely, excessive organic passivation can block active sites, reducing hydrogen peroxide activation efficiency in Fenton-like processes.

### Environmental Performance: Quantitative Comparison Heavy Metal Adsorption

The adsorption performance of biomass-derived iron oxide nanomaterials is governed by synergistic

interactions between iron surface hydroxyl groups and residual organic functional moieties originating from the biomass precursor. Surface ≡Fe–OH groups participate in inner-sphere complexation with metal cations such as Pb<sup>2+</sup> and Cd<sup>2+</sup> through ligand exchange mechanisms, while biomass-derived carboxylate and phenolic groups introduce additional coordination sites that enhance metal binding capacity (Zhang et al., 2016). Electrostatic attraction also contributes significantly, particularly when solution pH exceeds the point of zero charge (PZC), promoting favorable interactions between negatively charged surfaces and positively charged metal ions. In the case of redox-active species such as Cr(VI), partial reduction to Cr(III) may occur via Fe<sup>2+</sup>-mediated electron transfer, followed by immobilization through surface precipitation or complexation. Reported maximum adsorption capacities (q<sub>max</sub>) typically range from 30 to 250 mg g<sup>-1</sup> depending on pollutant type, surface functional density, and crystallographic phase. Removal efficiencies frequently exceed 80–99% under optimized pH conditions (generally pH 5–7 for divalent cations), highlighting the combined contribution of structural phase, particle size (10–60 nm), and organic surface chemistry in dictating adsorption thermodynamics and kinetics.

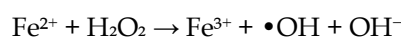
**Table 2.** Representative Adsorption Performance

Pollutant	q <sub>max</sub> (mg g <sup>-1</sup> )	Removal (%)	pH Range	Reference
Pb <sup>2+</sup>	80–250	90–99	5–7	(Abdul-Gafaru et al., 2025)
Cd <sup>2+</sup>	60–180	85–98	5–7	(Mohamed et al., 2023)
Cr(VI)	40–150	75–95	2–6	(Acharya & Parida, 2020)
As(V)	30–120	70–92	4–7	(Diephuis et al., 2022)

Variability is largely attributed to differences in surface functional group density and PZC shifts induced by biomass residues.

### Fenton-Like Catalytic Degradation

Catalytic performance is strongly phase-dependent. The classical reaction:



Mixed-valence Fe<sub>3</sub>O<sub>4</sub> systems demonstrate higher degradation kinetics due to continuous Fe<sup>3+</sup>/Fe<sup>2+</sup> cycling. Reported pseudo-first-order rate constants typically range from 0.02–0.15 min<sup>-1</sup>.

**Table 3.** Catalytic Degradation Performance

Pollutant	Phase	k (min <sup>-1</sup> )	Degradation (%)	H <sub>2</sub> O <sub>2</sub> (mM)
Methylene Blue (Bishnoi et al., 2018)	Fe <sub>3</sub> O <sub>4</sub>	0.05–0.15	90–100	5–20
Rhodamine B (Damasceno et al., 2024)	Fe <sub>3</sub> O <sub>4</sub> /γ-Fe <sub>2</sub> O <sub>3</sub>	0.03–0.10	85–98	10–30
Phenol (Bazrafshan et al., 2023)	γ-Fe <sub>2</sub> O <sub>3</sub>	0.02–0.06	70–90	10–25

Organic surface residues may either enhance Fe<sup>3+</sup> reduction (promoting redox cycling) or inhibit active site accessibility, depending on coating thickness.

### Photo-Fenton and Photocatalytic Systems

α-Fe<sub>2</sub>O<sub>3</sub> (bandgap ~2.1 eV) exhibits visible-light absorption but suffers from rapid charge recombination

(Saidani et al., 2025). In photo-Fenton systems, light-assisted Fe<sup>3+</sup> reduction improves radical generation and broadens operational pH range.

Defect-rich γ-Fe<sub>2</sub>O<sub>3</sub> and Fe<sub>3</sub>O<sub>4</sub> demonstrate enhanced charge transfer due to oxygen vacancies and mixed-valence structure. However, few studies quantify

quantum efficiency or long-term photostability (Xiang et al., 2025).

#### *Stability, Reusability, and Iron Leaching*

The long-term stability of biomass-derived iron oxide nanomaterials remains a critical determinant of their environmental applicability. Magnetite-dominant systems ( $\text{Fe}_3\text{O}_4$ ), although highly active in redox-driven processes, are thermodynamically susceptible to surface oxidation, gradually transforming into  $\gamma\text{-Fe}_2\text{O}_3$  under aerobic conditions or repeated catalytic cycles. This phase evolution reduces  $\text{Fe}^{2+}$  availability and weakens  $\text{Fe}^{3+}/\text{Fe}^{2+}$  redox cycling efficiency, thereby decreasing catalytic performance. Reported reusability studies commonly indicate a 5–20% decline in removal efficiency after 3–5 operational cycles, primarily due to partial oxidation, active site blockage by reaction intermediates, and structural aggregation. Iron leaching, particularly under acidic Fenton-like conditions (pH < 4), ranges from <1% to approximately 10% depending on reaction duration and surface coating stability. Biomass-derived organic layers may enhance colloidal stability and reduce aggregation through steric and electrostatic stabilization; however, excessive organic coverage can also weaken structural robustness and promote gradual Fe dissolution (Ahmad et al., 2019). Furthermore, repeated magnetic separation may induce mechanical aggregation, reducing accessible surface area. These findings underscore the necessity of phase monitoring, surface stabilization strategies, and standardized durability testing to ensure reproducible and scalable deployment in environmental remediation systems.

#### *Thermodynamic and Kinetic Considerations in Green Iron Oxide Formation*

The formation of iron oxide nanostructures in biomass-mediated systems is governed by coupled hydrolysis–condensation equilibria and redox-driven nucleation events. In aqueous systems,  $\text{Fe}^{3+}$  undergoes stepwise hydrolysis forming  $\text{Fe}(\text{OH})^{2+}$ ,  $\text{Fe}(\text{OH})_2^+$ , and ultimately  $\text{Fe}(\text{OH})_3$  species, whose supersaturation level dictates nucleation rates. Unlike conventional alkaline precipitation, biomass extracts modulate supersaturation through gradual  $\text{Fe}^{3+}$  reduction and chelation, effectively lowering the instantaneous nucleation burst and promoting controlled growth (Revathy et al., 2023).

From a thermodynamic perspective,  $\alpha\text{-Fe}_2\text{O}_3$  represents the most stable polymorph, whereas  $\text{Fe}_3\text{O}_4$  is metastable under oxidative conditions. The persistence of  $\text{Fe}_3\text{O}_4$  in green synthesis systems therefore reflects kinetic stabilization rather than thermodynamic preference. Organic ligands can lower surface energy by selective adsorption on specific crystallographic facets,

influencing anisotropic growth and particle morphology (Chakraborty et al., 2024).

Kinetic models reported across studies suggest pseudo-first-order growth behavior during early nucleation stages, while diffusion-controlled growth dominates at later times (Wroblewski et al., 2025). Reaction times between 30–180 minutes are commonly reported, with size increases observed beyond 120 minutes due to Ostwald ripening.

#### *Influence of Biomass Composition on Redox Pathways*

One of the defining variables in biomass-mediated iron oxide synthesis is the intrinsic chemical heterogeneity of the precursor extract, which directly governs redox equilibria, coordination dynamics, and nucleation pathways. Polyphenol-rich biomass containing tannins, catechins, and flavonoids exhibits stronger reducing capability due to phenolic hydroxyl groups capable of undergoing oxidation to quinone-like structures, thereby donating electrons to  $\text{Fe}^{3+}$  species through proton-coupled electron transfer mechanisms (Makarov et al., 2014). Depending on molecular structure, these phenolic systems display redox potentials typically ranging between +0.3 and +0.7 V versus SHE, sufficient to partially reduce  $\text{Fe}^{3+}$  to  $\text{Fe}^{2+}$  under mild thermal conditions. In contrast, carbohydrate-dominant biomass contributes weaker reducing capacity but provides steric stabilization through hydroxyl-rich polymeric chains. Organic acids such as citric, oxalic, and malic acids introduce additional complexity by forming  $\text{Fe}^{3+}$ -carboxylate complexes with stability constants (log K) commonly between 3 and 6, thereby modulating free  $\text{Fe}^{3+}$  activity and delaying hydrolysis-driven nucleation. This interplay between reduction kinetics and chelation strength determines the  $\text{Fe}^{2+}/\text{Fe}^{3+}$  ratio, defect density, and ultimately phase selectivity among  $\text{Fe}_3\text{O}_4$ ,  $\gamma\text{-Fe}_2\text{O}_3$ , and  $\alpha\text{-Fe}_2\text{O}_3$ . Consequently, even under comparable pH and temperature conditions, variations in biomass composition can yield markedly different crystallographic phases, magnetic responses, and catalytic efficiencies, representing a central challenge for reproducibility and cross-study comparability in green nanomaterial synthesis (Vindedahl et al., 2016).

This compositional variability underscores a fundamental limitation in current green synthesis protocols: the absence of chemical standardization of biomass extracts prior to nanoparticle formation. Most reported studies characterize the final iron oxide phase using XRD or magnetic measurements but rarely quantify the reducing capacity, total phenolic content, Fe-binding ligand density, or extract redox potential before synthesis. Without such pre-synthesis chemical profiling, correlations between biomass chemistry and final nanomaterial properties remain largely empirical.

Batch-to-batch fluctuations in phytochemical concentration, seasonal variation in biomass composition, and extraction conditions (temperature, solvent polarity, solid-to-liquid ratio) further amplify structural variability. As a consequence, similar synthesis parameters (pH 8–10, 60–80°C) may yield different  $\text{Fe}^{2+}/\text{Fe}^{3+}$  ratios and distinct phase distributions across laboratories. To improve reproducibility, future studies should incorporate quantitative extract characterization—such as total phenolic content assays, UV-Vis redox evaluation, or potentiometric measurements—alongside standardized reporting of Fe speciation and point of zero charge. Establishing such chemical benchmarks would enable predictive control over phase evolution and facilitate meaningful cross-study comparison in biomass-mediated iron oxide synthesis (Li et al., 2025).

#### *Magnetic Behavior and Structure–Magnetism Correlation*

Magnetic properties serve as indirect structural probes. Saturation magnetization ( $M_s$ ) values between 30–70  $\text{emu g}^{-1}$  are typically associated with  $\text{Fe}_3\text{O}_4$ -dominant systems, whereas  $\gamma\text{-Fe}_2\text{O}_3$  exhibits lower  $M_s$  (20–50  $\text{emu g}^{-1}$ ) due to vacancy ordering. Hematite ( $\alpha\text{-Fe}_2\text{O}_3$ ), being antiferromagnetic at room temperature, shows  $M_s$  values generally below 2  $\text{emu g}^{-1}$ .

Particle size strongly influences magnetic response. Superparamagnetic behavior is commonly observed below ~20 nm, eliminating magnetic remanence and preventing irreversible aggregation. However, excessive surface organic coverage reduces effective magnetization due to spin canting and non-magnetic mass contribution.

Magnetic recoverability is a key advantage in environmental remediation, enabling separation efficiencies above 90% within minutes using external magnets. Nevertheless, repeated magnetic cycling can induce aggregation, gradually lowering dispersibility and adsorption kinetics (Girardet et al., 2022).

#### *Comparative Assessment of Environmental Applications*

A cross-study comparison reveals that adsorption-based systems generally demonstrate broader pH tolerance (pH 4–8) compared to Fenton-based catalytic systems, which are often restricted to acidic conditions (pH 2–4). This distinction significantly affects practical deployment.

Heavy metal adsorption capacities (30–250  $\text{mg g}^{-1}$ ) are strongly influenced by surface functional density, whereas dye degradation efficiency correlates more strongly with  $\text{Fe}^{2+}$  availability and hydrogen peroxide concentration (5–30 mM typically reported). Rate constants (0.02–0.15  $\text{min}^{-1}$ ) suggest moderate catalytic kinetics compared to engineered synthetic magnetite,

indicating that surface passivation may partially limit electron transfer rates.

Few studies provide mineralization data (TOC removal), with most reporting only discoloration efficiency. This highlights a recurring limitation: performance metrics are often not standardized, hindering direct comparison across studies (Hoffmann et al., 2022).

#### *Reproducibility and Standardization Gaps*

Despite the growing number of studies reporting high removal efficiencies and promising magnetic recoverability, reproducibility remains a significant challenge in biomass-mediated iron oxide nanomaterial synthesis. Methodological inconsistencies are evident across the literature, particularly in the incomplete reporting of  $\text{Fe}^{2+}/\text{Fe}^{3+}$  ratios, absence of quantitative point of zero charge (PZC) measurements, and limited monitoring of phase evolution after repeated catalytic cycles. Many adsorption studies rely predominantly on Langmuir isotherm fitting without validating diffusion-controlled kinetic models, while catalytic degradation reports frequently omit radical scavenging experiments to confirm hydroxyl radical generation pathways. Furthermore, pollutant concentrations, oxidant dosages (e.g., 5–30 mM  $\text{H}_2\text{O}_2$ ), reaction volumes, and irradiation conditions in photo-assisted systems vary widely, hindering direct cross-study comparison. Iron leaching assessments are also inconsistently performed, even though reported dissolution rates may range from <1% to approximately 10% under acidic conditions. Without standardized benchmarking protocols—including uniform testing concentrations, consistent magnetic recovery evaluation, multi-cycle stability assessment beyond five cycles, and pre- and post-reaction structural characterization—performance claims remain difficult to generalize. Addressing these gaps is essential to transition biomass-derived iron oxide nanomaterials from laboratory-scale demonstrations toward reproducible, scalable, and regulatory-compliant environmental applications (Sharifi et al., 2022).

Collectively, the analyzed studies reveal that biomass-mediated synthesis of iron oxide nanomaterials is governed by tightly coupled redox–coordination equilibria that dictate phase evolution, defect chemistry, and surface functionality, ultimately controlling environmental performance. Magnetite-dominant systems exhibit superior redox-driven catalytic behavior due to  $\text{Fe}^{2+}/\text{Fe}^{3+}$  cycling, while surface-bound organic residues enhance adsorption capacity through additional coordination sites and electrostatic stabilization. However, these advantages are intrinsically linked to biomass compositional variability, which introduces significant heterogeneity in nucleation kinetics, crystalline phase distribution, and magnetic

response. Although removal efficiencies frequently exceed 80–99% and adsorption capacities may reach 250 mg g<sup>-1</sup> under optimized conditions, cross-study comparison remains constrained by inconsistent experimental parameters and insufficient chemical standardization. The field thus stands at a critical juncture: while mechanistic understanding has matured, reproducible synthesis control and unified performance benchmarking are still lacking. Bridging this gap requires quantitative extract characterization, systematic phase monitoring, and harmonized testing protocols to enable predictive design and scalable deployment of biomass-derived iron oxide nanomaterials in environmental remediation systems (de Oliveira et al., 2025).

## Conclusion

Biomass-mediated synthesis of iron oxide nanomaterials represents a promising sustainable strategy that integrates redox transformation, coordination chemistry, and surface functionalization into a single green synthetic platform. This review establishes an integrated structure–property–performance framework that systematically connects biomass phytochemistry, phase evolution, and functional environmental behavior of iron oxide nanomaterials. The analysis demonstrates that phase selectivity among Fe<sub>3</sub>O<sub>4</sub>, γ-Fe<sub>2</sub>O<sub>3</sub>, and α-Fe<sub>2</sub>O<sub>3</sub> is strongly governed by Fe<sup>3+</sup> reduction kinetics, ligand coordination strength, and hydrolysis-controlled nucleation, which collectively determine particle size, magnetic properties, and catalytic performance. Comparative evaluation highlights that Fe<sub>3</sub>O<sub>4</sub>-rich systems generally exhibit superior environmental functionality, with particle sizes of 10–30 nm, saturation magnetization values of 30–70 emu g<sup>-1</sup>, adsorption capacities up to 250 mg g<sup>-1</sup>, and pollutant removal efficiencies exceeding 90% under optimized conditions. In contrast, γ-Fe<sub>2</sub>O<sub>3</sub> and α-Fe<sub>2</sub>O<sub>3</sub> offer improved phase stability but lower magnetic responsiveness and redox efficiency. These findings provide critical insight into phase-dependent design strategies for targeted environmental applications, particularly in heavy metal adsorption and Fenton-based catalytic remediation. Beyond fundamental understanding, this review highlights important practical implications for industrial-scale nanomaterial production, including the valorization of biomass waste streams, reduction of chemical and energy inputs, and improved alignment with circular economy principles and sustainability regulations. Establishing standardized biomass characterization, phase-specific performance benchmarking, and stability assessment protocols will be essential to accelerate industrial translation and regulatory acceptance. Overall, this

work provides a mechanistic and quantitative foundation for developing more standardized, scalable, and sustainable iron oxide nanomaterials, supporting the next generation of environmentally responsible technologies for global water purification and pollutant remediation.

## Acknowledgments

The authors gratefully acknowledge the financial support provided by the Program Penelitian Fundamental under DRPM Satya Wacana Christian University contract number 049/SPK-PF/RIK/04/2025.

## Author Contributions

Conceptualization, D.K.A.K.; methodology, D.K.A.K.; software, D.K.A.K.; validation, D.K.A.K. and N.R.A.; formal analysis, D.K.A.K.; investigation, D.K.A.K., E.H.Y.S., and G.O.W.; resources, D.K.A.K. and A.R.G.; data curation, D.K.A.K.; writing—original draft preparation, D.K.A.K.; writing—review and editing, D.K.A.K. and N.R.A.; visualization, D.K.A.K.; supervision, N.R.A.; project administration, N.R.A.; funding acquisition, D.K.A.K. All authors have read and agreed to the published version of the manuscript.

## Funding

This research was funded by DRPM UKSW, grant number 049/SPK-PF/RIK/04/2025.

## Conflicts of Interest

The authors declare no conflict of interest.

## References

- Abdul-Gafaru, I., Cobbina, S. J., & Michael, K. (2025). Green-synthesized magnetic iron oxide nanoparticles for the adsorptive removal of Cd<sup>2+</sup> and Pb<sup>2+</sup> from aqueous solution. *Discover Water*, 5(1), 92. <https://doi.org/10.1007/s43832-025-00285-z>
- Abdullah, J. A. A., Lagos, S. N. P., Sanchez, E. J. E., Rivera-Flores, O., Sánchez-Barahona, M., Guerrero, A., & Romero, A. (2024). Innovative Agrowaste Banana Peel Extract-Based Magnetic Iron Oxide Nanoparticles for Eco-Friendly Oxidative Shield and Freshness Fortification. *Food and Bioprocess Technology*, 17(12), 5083–5096. <https://doi.org/10.1007/s11947-024-03423-y>
- Acharya, R., & Parida, K. (2020). A review on adsorptive remediation of Cr (VI) by magnetic iron oxides and their modified forms. *Biointerface Research in Applied Chemistry*, 10(2), 5266–5272. <https://doi.org/10.33263/BRIAC102.266272>
- Ahmad, T., Phul, R., & Khan, H. (2019). Iron Oxide Nanoparticles: An Efficient Nano-catalyst. *Current Organic Chemistry*, 23(9), 994–1004. <https://doi.org/10.2174/138527282366619031415>

3208

- Alex Mbachu, C., Kamoru Babayemi, A., Chinedu Egbosiuba, T., Ifeanyichukwu Ike, J., Jacinta Ani, I., & Mustapha, S. (2023). Green synthesis of iron oxide nanoparticles by Taguchi design of experiment method for effective adsorption of methylene blue and methyl orange from textile wastewater. *Results in Engineering*, *19*, 101198. <https://doi.org/10.1016/j.rineng.2023.101198>
- Bazrafshan, E., Mohammadi, L., Zarei, A. A., Mosafer, J., Zafar, M. N., & Dargahi, A. (2023). Optimization of the photocatalytic degradation of phenol using superparamagnetic iron oxide (Fe<sub>3</sub>O<sub>4</sub>) nanoparticles in aqueous solutions. *RSC Advances*, *13*(36), 25408–25424. <https://doi.org/10.1039/D3RA03612J>
- Bishnoi, S., Kumar, A., & Selvaraj, R. (2018). Facile synthesis of magnetic iron oxide nanoparticles using inedible *Cynometra ramiflora* fruit extract waste and their photocatalytic degradation of methylene blue dye. *Materials Research Bulletin*, *97*, 121–127. <https://doi.org/10.1016/j.materresbull.2017.08.040>
- Castillo, J., Vargas, V., Macero, D., Le Beulze, A., Ruiz, W., & Bouyssiére, B. (2021). One-step synthesis of SiO<sub>2</sub> α-Fe<sub>2</sub>O<sub>3</sub> / Fe<sub>3</sub>O<sub>4</sub> composite nanoparticles with magnetic properties from rice husks. *Physica B: Condensed Matter*, *605*, 412799. <https://doi.org/10.1016/j.physb.2020.412799>
- Chakraborty, A. R., Zohora Toma, F. T., Alam, K., Yousuf, S. B., & Hossain, K. S. (2024). RETRACTED: Influence of annealing temperature on Fe<sub>2</sub>O<sub>3</sub> nanoparticles: Synthesis optimization and structural, optical, morphological, and magnetic properties characterization for advanced technological applications. *Heliyon*, *10*(21), e40000. <https://doi.org/10.1016/j.heliyon.2024.e40000>
- Damasceno, B. S., da Silva, V. C., Rodrigues, A. R., Falcão, E. H. L., & Vaz de Araújo, A. C. (2024). Use of magnetic nanoparticles of iron oxide and their derivatives in the adsorption of rhodamine 6G and rhodamine B dyes. *Journal of Alloys and Compounds*, *1005*, 175907. <https://doi.org/10.1016/j.jallcom.2024.175907>
- de Oliveira, M. L., Cancino-Bernardi, J., & da Veiga, M. A. M. S. (2025). Understanding and predicting the environmental dispersion of iron oxide nanoparticles: a comprehensive study on synthesis, characterisation, and modelling. *Environmental Science: Nano*, *12*(1), 791–804. <https://doi.org/10.1039/D3EN00860F>
- Demirezen, D. A., Yilmaz, Ş., Yilmaz, D. D., & Yıldız, Y. Ş. (2022). Green synthesis of iron oxide nanoparticles using *Ceratonia siliqua* L. aqueous extract: improvement of colloidal stability by optimizing synthesis parameters, and evaluation of antibacterial activity against Gram-positive and Gram-negative bacteria. *International Journal of Materials Research*, *113*(10), 849–861. <https://doi.org/10.1515/ijmr-2022-0037>
- Devi, S. M., Nivetha, A., & Prabha, I. (2019). Superparamagnetic Properties and Significant Applications of Iron Oxide Nanoparticles for Astonishing Efficacy—a Review. *Journal of Superconductivity and Novel Magnetism*, *32*(2), 127–144. <https://doi.org/10.1007/s10948-018-4929-8>
- Diephuis, W. R., Molloy, A. L., Boltz, L. L., Porter, T. B., Aragon Orozco, A., Duron, R., Crespo, D., George, L. J., Reiffer, A. D., Escalera, G., Bohoulou, A., Avendano, C., Colvin, V. L., & Gonzalez-Pech, N. I. (2022). The Effect of Agglomeration on Arsenic Adsorption Using Iron Oxide Nanoparticles. *Nanomaterials*, *12*(9), 1598. <https://doi.org/10.3390/nano12091598>
- Dong, H., Du, W., Dong, J., Che, R., Kong, F., Cheng, W., Ma, M., Gu, N., & Zhang, Y. (2022). Depletable peroxidase-like activity of Fe<sub>3</sub>O<sub>4</sub> nanozymes accompanied with separate migration of electrons and iron ions. *Nature Communications*, *13*(1), 5365. <https://doi.org/10.1038/s41467-022-33098-y>
- Girardet, T., Venturini, P., Martinez, H., Dupin, J.-C., Cleymand, F., & Fleutot, S. (2022). Spinel Magnetic Iron Oxide Nanoparticles: Properties, Synthesis and Washing Methods. *Applied Sciences*, *12*(16), 8127. <https://doi.org/10.3390/app12168127>
- Hoffmann, N., Tortella, G., Hermosilla, E., Fincheira, P., Diez, M. C., Lourenço, I. M., Seabra, A. B., & Rubilar, O. (2022). Comparative Toxicity Assessment of Eco-Friendly Synthesized Superparamagnetic Iron Oxide Nanoparticles (SPIONs) in Plants and Aquatic Model Organisms. *Minerals*, *12*(4), 451. <https://doi.org/10.3390/min12040451>
- Hu, Y., Han, X., Zhang, N., Guo, L., & Zhang, L. (2025). Insight into the performance and mechanism of Iron(II, III)-polyphenol particles on the adsorption of malachite green cationic dye. *Scientific Reports*, *15*(1), 39056. <https://doi.org/10.1038/s41598-025-26499-8>
- Khan, M. A., Ahmed, M., Abu-Hussien, S. H., Zahid, M. U., & Alharbi, B. F. (2025). Green synthesis of iron oxide nanoparticles (Fe<sub>2</sub>O<sub>3</sub>-NPs) from Citrus Limetta agrowaste for biological and photocatalytic applications. *Scientific Reports*, *15*(1), 33107. <https://doi.org/10.1038/s41598-025-17750-3>
- Kumar, V., Kaushik, N. K., Tiwari, S. K., Singh, D., & Singh, B. (2023). Green synthesis of iron nanoparticles: Sources and multifarious

- biotechnological applications. *International Journal of Biological Macromolecules*, 253, 127017. <https://doi.org/10.1016/j.ijbiomac.2023.127017>
- Li, Z., Gou̇t, T. L., Zhang, J., Zhao, J., Liu, J., & Hu, Y. (2025). Review on stability of iron (oxyhydr)oxide nanoparticles in natural environments: interactions with metals, organics, and microbes. *Environmental and Biogeochemical Processes*, 1(1), 0–0. <https://doi.org/10.48130/ebp-0025-0013>
- Magomedova, A., Isaev, A., Orudzhev, F., Sobola, D., Murtazali, R., Rabadanova, A., Shabanov, N. S., Zhu, M., Emirov, R., Gadzhimagomedov, S., Alikhanov, N., & Kasinathan, K. (2023). Magnetically Separable Mixed-Phase  $\alpha/\gamma$ -Fe<sub>2</sub>O<sub>3</sub> Catalyst for Photo-Fenton-like Oxidation of Rhodamine B. *Catalysts*, 13(5), 872. <https://doi.org/10.3390/catal13050872>
- Makarov, V. V., Makarova, S. S., Love, A. J., Sinitsyna, O. V., Dudnik, A. O., Yaminsky, I. V., Taliany, M. E., & Kalinina, N. O. (2014). Biosynthesis of Stable Iron Oxide Nanoparticles in Aqueous Extracts of *Hordeum vulgare* and *Rumex acetosa* Plants. *Langmuir*, 30(20), 5982–5988. <https://doi.org/10.1021/la5011924>
- Malacaria, L., Corrente, G. A., Beneduci, A., Furia, E., Marino, T., & Mazzone, G. (2021). A Review on Coordination Properties of Al(III) and Fe(III) toward Natural Antioxidant Molecules: Experimental and Theoretical Insights. *Molecules*, 26(9), 2603. <https://doi.org/10.3390/molecules26092603>
- Mohamed, A., Atta, R. R., Kotp, A. A., Abo El-Ela, F. I., Abd El-Raheem, H., Farghali, A., Alkhalifah, D. H. M., Hozzein, W. N., & Mahmoud, R. (2023). Green synthesis and characterization of iron oxide nanoparticles for the removal of heavy metals (Cd<sup>2+</sup> and Ni<sup>2+</sup>) from aqueous solutions with Antimicrobial Investigation. *Scientific Reports*, 13(1), 7227. <https://doi.org/10.1038/s41598-023-31704-7>
- Nehe, A. D., & Kulkarni, A. D. (2025). Fundamentals of Superparamagnetic Iron Oxide Nanoparticles: Recent Update. *Journal of Microscopy and Ultrastructure*, 13(3), 113–129. [https://doi.org/10.4103/jmau.jmau\\_17\\_22](https://doi.org/10.4103/jmau.jmau_17_22)
- Parveen, S., Riyazur Rahman, F., Thulasi Krishnan, S., Kalaiarasi, G., Dinesh, A., Srimathi Priya, L., Gnanasekaran, L., Santhamoorthy, M., Ayyar, M., & Santhoshkumar, S. (2025). Green Synthesis of Metal Oxide Nanoparticles via Plant Extracts for Biological Applications: A Review. *Trends in Sciences*, 22(6), 9592. <https://doi.org/10.48048/tis.2025.9592>
- Periakaruppan, R., Chen, X., Thangaraj, K., Jeyaraj, A., Nguyen, H. H., Yu, Y., Hu, S., Lu, L., & Li, X. (2021). Utilization of tea resources with the production of superparamagnetic biogenic iron oxide nanoparticles and an assessment of their antioxidant activities. *Journal of Cleaner Production*, 278, 123962. <https://doi.org/10.1016/j.jclepro.2020.123962>
- Ramos-Guivar, J. A., Flores-Cano, D. A., & Caetano Passamani, E. (2021). Differentiating Nanomaghemite and Nanomagnetite and Discussing Their Importance in Arsenic and Lead Removal from Contaminated Effluents: A Critical Review. *Nanomaterials*, 11(9), 2310. <https://doi.org/10.3390/nano11092310>
- Revathy, R., Sajini, T., Augustine, C., & Joseph, N. (2023). Iron-based magnetic nanomaterials: Sustainable approaches of synthesis and applications. *Results in Engineering*, 18, 101114. <https://doi.org/10.1016/j.rineng.2023.101114>
- Saidani, M. A., Fkiri, A., Chouk, W., Altalhi, T., & Mezni, A. (2025). Synthesis, Characterization and Photocatalytic Evaluation of Multifunctional Ternary Au@ZnO/ $\alpha$ -Fe<sub>2</sub>O<sub>3</sub> Nanocomposite for Organic Pollutant Removal. *Water, Air, & Soil Pollution*, 236(10), 644. <https://doi.org/10.1007/s11270-025-08301-7>
- Shabatina, T. I., Vernaya, O. I., Shabatin, V. P., & Melnikov, M. Y. (2020). Magnetic Nanoparticles for Biomedical Purposes: Modern Trends and Prospects. *Magnetochemistry*, 6(3), 30. <https://doi.org/10.3390/magnetochemistry603030>
- Sharifi, S., Mahmoud, N. N., Voke, E., Landry, M. P., & Mahmoudi, M. (2022). Importance of Standardizing Analytical Characterization Methodology for Improved Reliability of the Nanomedicine Literature. *Nano-Micro Letters*, 14(1), 172. <https://doi.org/10.1007/s40820-022-00922-5>
- Tiwari, S., Bhargawa, P. K., & Kumar, R. (2026). Biomass-mediated nanomaterials for petroleum refinery waste remediation: a comprehensive review of mechanisms and applications. *Environmental Monitoring and Assessment*, 198(1), 77. <https://doi.org/10.1007/s10661-025-14803-y>
- Tricco, A. C., Lillie, E., Zarin, W., O'Brien, K. K., Colquhoun, H., Levac, D., Moher, D., Peters, M. D. J., Horsley, T., Weeks, L., Hempel, S., Akl, E. A., Chang, C., McGowan, J., Stewart, L., Hartling, L., Aldcroft, A., Wilson, M. G., Garritty, C., ... Straus, S. E. (2018). PRISMA Extension for Scoping Reviews (PRISMA-ScR): Checklist and Explanation. *Annals of Internal Medicine*, 169(7), 467–473. <https://doi.org/10.7326/M18-0850>
- Tyagi, N., Gupta, P., Khan, Z., Neupane, Y. R., Mangla, B., Mehra, N., Ralli, T., Alhalmi, A., Ali, A., Al

- Kamaly, O., Saleh, A., Nasr, F. A., & Kohli, K. (2023). Superparamagnetic Iron-Oxide Nanoparticles Synthesized via Green Chemistry for the Potential Treatment of Breast Cancer. *Molecules*, 28(5), 2343. <https://doi.org/10.3390/molecules28052343>
- Vindedahl, A. M., Strehlau, J. H., Arnold, W. A., & Penn, R. L. (2016). Organic matter and iron oxide nanoparticles: aggregation, interactions, and reactivity. *Environmental Science: Nano*, 3(3), 494–505. <https://doi.org/10.1039/C5EN00215J>
- Wang, P., Zhou, X., Zhang, Y., Yang, L., Zhi, K., Wang, L., Zhang, L., & Guo, X. (2017). Unveiling the mechanism of electron transfer facilitated regeneration of active Fe 2+ by nano-dispersed iron/graphene catalyst for phenol removal. *RSC Advances*, 7(43), 26983–26991. <https://doi.org/10.1039/C7RA04312K>
- Wang, W., Liu, Y., Yue, Y., Wang, H., Cheng, G., Gao, C., Chen, C., Ai, Y., Chen, Z., & Wang, X. (2021). The Confined Interlayer Growth of Ultrathin Two-Dimensional Fe<sub>3</sub>O<sub>4</sub> Nanosheets with Enriched Oxygen Vacancies for Peroxymonosulfate Activation. *ACS Catalysis*, 11(17), 11256–11265. <https://doi.org/10.1021/acscatal.1c03331>
- Wroblewski, C., Ravikumar, S. P., Barbhuiya, R. I., Raveendran Nair, G., Elsayed, A., & Singh, A. (2025). A novel magnetically separable <math>pH</math> sensitive surface-active iron oxide nanoparticles for the removal of antibiotics (tetracycline) from aquatic environments. *The Canadian Journal of Chemical Engineering*, 103(11), 5373–5385. <https://doi.org/10.1002/cjce.25722>
- Xiang, T., Cai, X., Luo, Z., Zhou, X., Yan, C., Yu, J., Ge, J., & Li, Y. (2025). Defect engineering to boost charge transfer of Mn-doped  $\gamma$ -Fe<sub>2</sub>O<sub>3</sub> hollow porous microspheres via O/Fe Mn charge channel for efficient photo-Fenton degradation of organics. *Journal of Alloys and Compounds*, 1019, 179269. <https://doi.org/10.1016/j.jallcom.2025.179269>
- Xu, W., Yang, T., Liu, S., Du, L., Chen, Q., Li, X., Dong, J., Zhang, Z., Lu, S., Gong, Y., Zhou, L., Liu, Y., & Tan, X. (2022). Insights into the Synthesis, types and application of iron Nanoparticles: The overlooked significance of environmental effects. *Environment International*, 158, 106980. <https://doi.org/10.1016/j.envint.2021.106980>
- Yousif, N., Al-Jawad, S., Taha, A., & Stamatis, H. (2023). A review of Structure, Properties, and Chemical Synthesis of Magnetite Nanoparticles. *Journal of Applied Sciences and Nanotechnology*, 3(2), 18–31. <https://doi.org/10.53293/jasn.2022.5179.1178>
- Zhang, C., Yu, Z., Zeng, G., Huang, B., Dong, H., Huang, J., Yang, Z., Wei, J., Hu, L., & Zhang, Q. (2016). Phase transformation of crystalline iron oxides and their adsorption abilities for Pb and Cd. *Chemical Engineering Journal*, 284, 247–259. <https://doi.org/10.1016/j.cej.2015.08.096>